# Numerical modelling of desiccation crack induced permeability

## Modélisation numérique de la perméabilité induite par la fissuration des sols

Stirling R.A., Davie C.T., Glendinning S.
*Newcastle University, Newcastle-upon-Tyne, UK*

ABSTRACT: The development of cracking as a result of desiccation and the apparent increase in permeability of cracked fill is increasingly under investigation. Rainfall infiltration into soil surfaces that experience cracking increases due to the additional, preferential transmission of water. This in turn results in cycles of rapidly elevated pore water pressure and is widely cited as a significant mechanism for strength reduction that leads to embankment failure. A two-phase flow numerical model that allows the partially saturated behaviour of the desiccated medium to be captured is presented based on the finite difference code FLAC 2D. The material properties of the developed model, including soil stiffness and strength, are incorporated as a function of drying. The model has allowed investigation into the factors influencing the incidence and scale of cracking.

RÉSUMÉ : L'infiltration des précipitations dans les sols sensibles à la dessiccation augmente comme résultat de la transmission préférentielle, additionnelle d'eau. Ce phénomène se traduit par des cycles de pression interstitielle rapidement élevée, et est largement cité comme un mécanisme important de la réduction de la résistance qui conduit à la rupture des remblais. Un modèle numérique de l'écoulement diphasique, permettant la prise en compte du comportement partiellement saturé du milieu desséché, est présenté. Ce modèle est basé sur un code de calcul de différences finies, FLAC 2D. Les propriétés du matériau du modèle, y compris la rigidité et la résistance du sol, sont incorporées comme fonction du séchage dans la description de la courbe caractéristique sol-eau. Le modèle a permis également l'évaluation des principaux facteurs qui influencent l'incidence et l'ampleur de la fissuration des sols.

KEYWORDS: Numerical modelling, Unsaturated soils, Soil behaviour

## 1 INTRODUCTION

Cracking within clay fills has been an accepted phenomenon for many decades. The engineering study of desiccation cracking has been motivated by its impact upon the effectiveness of many earth structures including liners (Philip et al 2002), foundations (Silvestri et al 1992), cuttings and embankments (Smethurst et al 2006) due to an apparent increase in water infiltration.

Desiccation cracking is the product of volumetric shrinking of clays brought about by a reduction in soil-water content. Cracking initiates when tensile stresses generated by increasing suctions exceed the soil strength, which in itself, is controlled by soil water content. Variability in soil-water content is primarily the result of seasonal fluctuation in precipitation/evaporation in addition to the transient demands of vegetation and the infiltration potential of the soil surface and is therefore largely governed by climate.

Predicted climate change scenarios are recognised to have the capacity to more frequently bring about conditions conducive to the increased occurrence of this behaviour because of the increased occurrence of warmer and drier summers experiencing rainfall events of shorter duration and higher intensity (Hulme et al 2002, Jenkins et al 2010).

Progressive failure is thought to be largely governed by permeability which is in turn controlled by the micro- and macro-scale structure of the soil. Previous studies have established that current permeability measurement techniques produce discrepancies between both laboratory and field established values and numerically simulated pore-water pressure values (Smethurst et al 2006, Rouainia et al 2009). These differences have been identified as being caused by permeability values ranging by up to three orders of magnitude (Nyambayo and Potts 2005, Rouainia et al 2009). Albrecht and Benson (2001) identified the same increase in hydraulic conductivity of three orders of magnitude in laboratory testing of small cracked samples when compared to equivalent non-cracked samples of the same material. This supports the notion that it is the presence of pervasive cracks that results in the elevated permeability. An empirically reasoned permeability modification has been employed in the modelling of embankment pore pressures (Nyambayo et al 2004).

Many researchers have attempted to model the mechanisms involved in crack initiation and propagation, particularly with respect to crack pattern. Kodikara and Choi (2006) present a simplified analytical model for laboratory cracking which has subsequently been implemented by Amarasiri et al. (2011) into a distinct element code. Their work describes the modelling of cracking behaviour in slurried clays under given laboratory boundary conditions and incorporates material changes due to drying. More recently, work has been carried out using the finite element method to investigate the development of tensile stresses associated with desiccation (Trabelsi et al 2011, Peron et al 2012). In contrast, this work models partially saturated flow throughout the medium induced by a simulated evaporation boundary and combines this mechanism with the ability to capture a fracturing geometry.

## 2 TWO-PHASE FLOW

Modelling has been carried out using the commercial finite difference code, FLAC (Fast Lagrangian Analysis of Continua) (ITASCA, 2002). The internal programming language, FISH, has allowed material variables to be defined as a function of water content. Given the fundamental influence of water content in desiccation cracking, it is important to be able to capture the partially saturated behaviour of the medium. To do this, the Two-phase Flow (tp-flow) option available with FLAC was used.

The tp-flow option allows the flow of two immiscible fluids to be modelled whose proportions are representative of soil saturation. Darcy's law is then used to define the wetting and non-wetting fluid flow according to their relative pressures. Capillary pressure is fundamentally linked to the effective saturation and is considered in this work using the van Genuchten approximation (van Genuchten 1980). The relative permeability of each fluid is considered to be a fraction of the saturated coefficient of permeability dependent upon the effective saturation.

Coupled fluid-mechanical modelling was conducted in which volumetric deformation causes changes in fluid pressures. Similarly, changes in effective stress result in volumetric strain, with the pore pressure increment weighted by the level of saturation (Itasca 2002).

## 3 MATERIAL PROPERTIES

### 3.1 Continuum properties

For simplicity, the soil was assumed to behave elastically, although non-linear behaviour was captured as described below. Young's Modulus, $E$ (MPa), in partially saturated soils is a function of water content, $\omega$ (%), this relationship was derived experimentally for the material modelled using constant water triaxial tests. These data are presented in Figure 1.

The properties required by the software were dry density, bulk and shear moduli. The bulk and shear moduli were calculated using the Young's modulus from Figure 1 and a Poisson's ratio of 0.3 (Tomlinson 2001). These moduli were updated at each time-step of the analysis using code developed in FISH and were based on changes in element water content. The initial dry density of the soil was 1.65Mg/m$^3$, based upon sampling of a full scale trial embankment at Newcastle University (Hughes et al 2007).

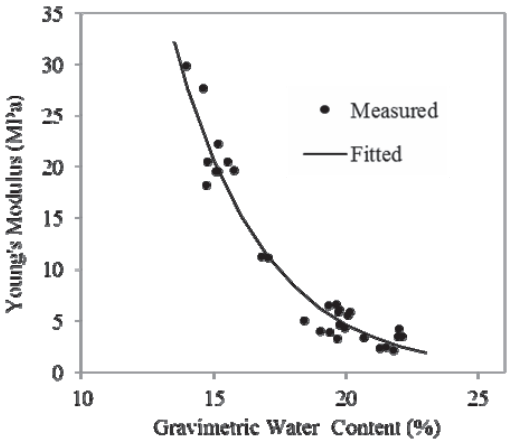


Figure 1 The trend in Young's modulus at varying water content.

### 3.2 Interface properties

Interfaces were sited vertically throughout the mesh with regular spacing. The use of interfaces enables separation of the mesh into discrete regions between which slip and separation can occur, subject to criteria set by interface properties and so provide locations for potential cracking.

The Interface bond will break when tensile stresses exceed the tensile strength or when shear stresses exceed the shear strength of the individual interface. Separation can then occur along the interface segment (delineated by node pairs) where this condition is met.

The interface properties comprise the friction angle; cohesion; tensile strength and stiffness in both the normal and shear orientations. Interface property values were derived primarily from standard laboratory tests (e.g. direct shear test). However, interface normal and shear stiffness were calculated according to the relative stiffness and size of neighbouring elements. As with continuum stiffness, interface stiffness was updated while stepping using the relationship with water content.

The magnitude of tensile strength for a given soil is widely recognised to be dependent upon the soil water content and therefore, suction present (Heibrock et al 2003, Nahlawi et al 2004, Tamrakar et al 2005, Trabelsi et al 2011). Laboratory testing was conducted using an adapted standard direct shear apparatus on samples of the modelled clay at varying water content. The identified trend input to the model is presented in Figure 2.

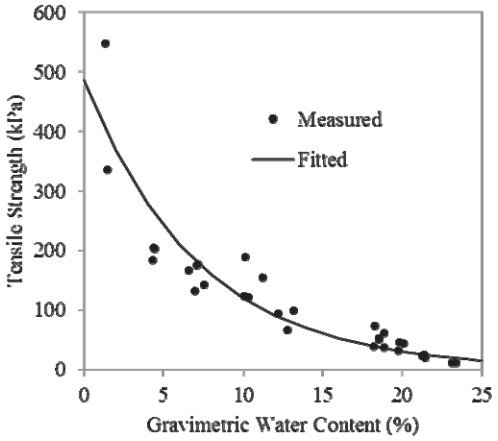


Figure 2 Tensile strength of compacted clay as a function of water content.

In addition to the dependency of interface tensile strength with water content, variability in soil strength was also included using a normally distributed random number facility about the experimentally derived value. This variability was included to enable a degree of the inherent heterogeneity of compacted clay to be better captured. The implications of this method on crack initiation and spacing is discussed later.

Restrained shrinkage at the base of clay has been shown to have a great influence on the generation of the tensile stress that leads to cracking (Peron, et al., 2009). The clay-mould interface properties incorporated were based upon laboratory trials of compacted clay shrinkage in specially constructed moulds.

### 3.3 Hydrological Properties

To implement the two-phase flow calculation, van Genuchten properties of the clay were obtained from the soil water retention curve established using the Filter Paper Technique. These data are presented in Figure 3 alongside the implemented fitted van Genuchten approximation.

The curve describes the general trend of increasing suction with decreasing soil water content. It is this increase in suction that is understood to bring about an increase in soil stiffness and strength, in addition to shrinkage strain required for the development of tensile stress.

The saturated mobility coefficient input to FLAC was calculated from the coefficient of permeability and the dynamic viscosity of water. The permeability value used was measured from un-cracked sites on a trial embankment constructed using the modelled clay fill (Hughes et al 2007).

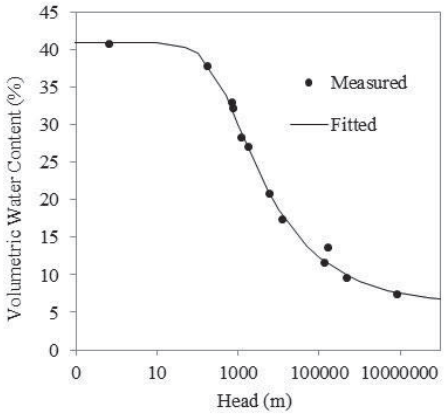


Figure 3 Soil water characteristic curve.

## 4 NUMERICAL MODEL

The model developed in this work was based on experiments conducted to investigate the desiccation cracking of compacted clay fill in the laboratory. As such, the geometry (Figure 4), material behaviour and initial conditions were based on these experiments.

The modelled mould consisted of a 190x2 element thick region located beneath the mesh representing the clay and was fixed in space. The remaining mesh comprised 190x17 quadrilateral elements, 94 vertically orientated interfaces and 95 horizontal interfaces, the latter forming a single plane between the base of the clay mesh and the mould. All boundaries of the sample mesh remained free to shrink/swell in any orientation. Plane-stress was configured given the finite out-of-plane depth of the modelled scenario.

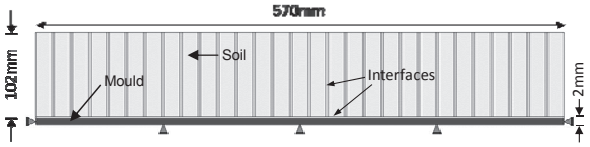


Figure 4 Geometry of the model mesh.

An evaporative drying condition was applied to the exposed, upper surface of the clay. The drying flux was numerically simulated by application of a discharge boundary condition statically located at the upper surface of the model mesh (5a).

During the early stages of experimental drying, shrinkage was observed as both ends of the soil sample, away from the mould ends resulting in an increase in the exposed surface area of the sample. Therefore, in addition to simulated discharge from the upper surface of the sample mesh, the transient behaviour of the exposed end surfaces was accommodated. Furthermore, the evaporative surface area increases upon the onset of cracking and this is also included. At every simulated hour of drying, each interface is assessed for separation (i.e. crack opening). When separation is identified, the exposed 'crack wall' is subjected to the dynamic discharge condition. An example evolution of the drying boundary geometry is illustrated in Figure 5.

The model requires a drying rate to be applied to the surface, this was determined from laboratory experiments where mass loss is considered to be solely that of water.

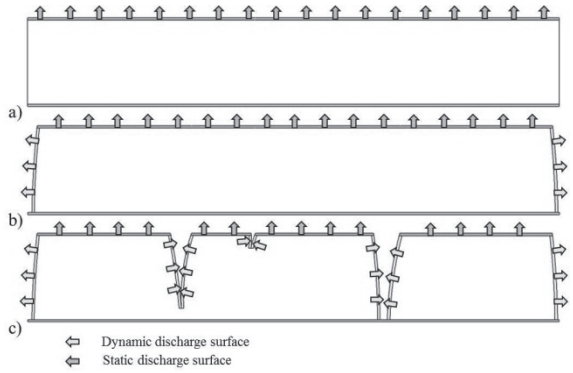


Figure 5 Illustration of the drying boundaries a) Initial upper surface b) Upper surface plus exposed sample ends and c) Upper surface, exposed ends plus crack walls.

## 5 RESULTS

An example of the output geometry from a typical simulation is provided in Figure 6a alongside a representative laboratory experiment. It can be seen that shrinkage of the modelled clay has taken place, represented by the difference in total length between the mesh simulating the clay and that of the fixed mould. Towards the outer boundaries of the clay mesh, the edge is seen to curve from the vertical. This realistic behaviour is captured by the ability of the model to generate the non-linear negative pore pressure gradient through the depth of the mesh. By applying a drying condition to the outer surface, primarily the upper boundary, this region has been found to develop the greatest suction magnitudes. Additionally, the overall residual height of the mesh following drying is found to have reduced from the pre-drying condition.

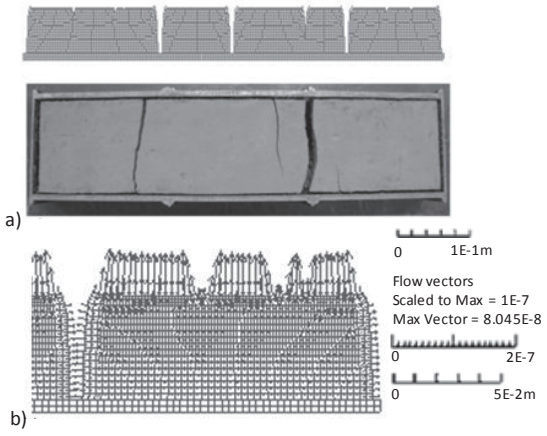


Figure 6 a) Model geometry output (side elevation) and an inset example laboratory experiment (plan elevation) and b) Cracked geometry with flow vectors.

Flow may be seen in Figure 6b to predominantly act in the upward direction throughout the medium. In the vicinity of separated interfaces, flow is shown to occur toward the crack wall contributing to the overall drying mechanism of the model.

The ability to capture the development of tensile stress throughout the medium is vital for the simulation of crack initiation and growth conditions. A representative contour plot of total horizontal stress is presented in Figure 7. Most clearly depicted is the generation of greatest tensile stress localisation about the modelled crack tip. As the propagation of interface separation takes place it is found that the magnitude of this

stress concentration increases. However, upon full separation of the mesh, this tip stress is relieved as propagation is halted. The mesh is then free to shrink further subject to the basal friction condition.

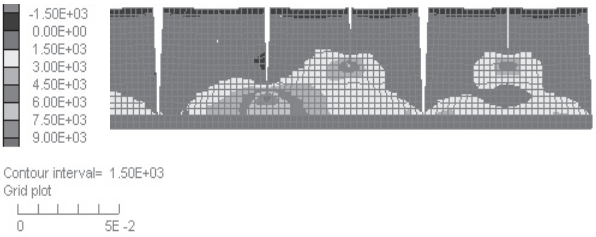


Figure 7 Distribution of total stress in the horizontal orientation.

The formation of shallow compressive stress concentrations at the upper surface, such as that shown between existing cracks in Figure 7 is considered to be the indicator of crack initiation loci. The progressive development of such surface stress concentrations away from previous crack formation is evidence of sequential crack formation. The incorporation of tensile strength variability across the many interfaces has allowed this phenomenon not to dominate, therefore avoiding symmetry in the resultant crack pattern. Simultaneous growth of primary cracking at spacing relative to the progressive development of surface stress is evident in Figure 6a, shown by the fully penetrating cracks. The initiation of minor cracks at the surface has led to stress relaxation and inhibited further pervasive cracking.

Growth of basal tensile stress concentrations are shown to result from the imposed shear conditions at the clay-mould interface. These are found to contribute to the propagation of interface separation approaching the base of the clay. However, clay tensile strength is consistently exceeded at the evaporative outer boundary initially.

## 6 CONCLUSIONS

This work is set in the context of cracking due to seasonal drying in compacted, engineered fills used in the construction of infrastructure embankments.

The model presented is capable of replicating the non-linear, partially saturated state that results from the application of a drying flux. Through incorporating interface elements, the model is not only able to model the stress field generated through drying but is capable of simulating the cracking behaviour of an engineered fill undergoing desiccation. It is recognised that the placement of predefined, potential cracking sites has the inherent tendency to bias the distribution of cracking. However, attempts have been made to include a degree of heterogeneity in tensile strength throughout a finely discretised mesh. Through this, a combination of spontaneous and sequential crack initiation processes is captured much like the development of primary and second order cracking recorded in the field.

The use of a dynamic, evaporative boundary condition is incorporated in an attempt to capture the transient nature of surface permeability under drying.

## 7 ACKNOWLEDGEMENTS

The authors would like to thank Stuart Patterson for help with laboratory work, Dr Joao Mendes for triaxial data and Dr Peter Helm for his helpful advice in the use of the numerical software.

## 8 REFERENCES

Albrecht B. A. and Benson C. H. 2001 Effect of desiccation on compacted natural clays. *J. Geotechnical and Geoenvironmental Eng.* 127 (1), 67-75

Amarasiri A. L., Kodikara J. K. and Costa S. 2011 Numerical modelling of desiccation cracking. *Int. J. Numerical and Analytical Methods in Geomech.* 35, 82-96

Heibrock G, Zeh, R. M. and Witt K. J. 2003 Tensile strength of compacted clays. *Preceedings of the international conference 'From Experimental Evidence towards Numerical Modelling of Unsaturated Soils.* Weimar, Germany

Hughes P., Glendinning S. and Mendes J. 2007 Construction, testing and instrumentation of an infrastructure testing embankment. *Proceedings of the Expert Symposium on Climate Change Modelling, Impacts & Adaptations,* Singapore, 159-166

Hulme M., Jenkins G. J., Lu X., Turnpenny J. R., Mitchell T. D., Jones R. G., Lowe J., Murphy J. M., Hassell D., Boorman P., McDonald R. and Hill S. 2002 Climate change scenarios for the United Kingdom: The UKCIP02 Scientific Report, Tyndall Centre for climate change research, Norwich

ITASCA 2002 FLAC User's Guide. ITASCA, Minnesota

Jenkins G., Murphy J., Sexton D., Lowe J., Jones P. and Kilsby C. 2010 UK climate projections: Briefing report. 2. UK Climate Impacts Programme

Kodikara J. K. and Choi X. 2006 A simplified analytical model for desiccation cracking of clay layers in laboratory tests. *ASCE Geotechnical Special Publication* 2, 2558-2569

Nahlawi H., Charkrabarti S. and Kodikara J. 2004 A direct tensile strength testing method for unsaturated geomaterials. *ASTM Geotechnical Testing Journal*. 27 (4), 1-6

Nyambayo V. P. and Potts D. M. 2005 A new permeability model for shrinkable soils undergoing desiccation. *Proceedings of the International Conference on Soil Mech. and Geotechnical Eng.* 2, 831-836

Nayambayo V. P., Potts D. M. and Addenbrooke T. I. 2004 The influence of permeability on the stability of embankments experiencing seasonal pore water pressure changes. *Advances in Geotechnical Eng.: The Skempton Conference,* Thomas Telford, London, 898-910

Peron H., Laloui L., Hu B. L. and Hueckel T. 2012 Formatio of drying crack patterns in soils: a deterministic approach. Acta Geotechnica, 1-7

Peron H., Hueckel L., Laloui L. and Hu L. B. 2009 Fundamentals of desiccation cracking of fine-grained soils: experimental characterisation and mechanisms identification. *Can. Geotechnical J.* 46, 1177-1201

Philip L. K., Shimell H., Hewitt P. J. and Ellard H. T. 2002 A field-based test cell examining clay desiccation in landfill liners. *Q. J. Eng. Geol. and Hydrol*. 35, 345-354

Rouainia M., Davies O., O'Brien T. & Glendinning S. 2009 Numerical modelling of climate effects on slope stability. *Eng. Sustainability*, 162 (ES2), 81-89

Silvestri V., Sarkis G., Bekkouche N. and Soulie M. 1992 Evapotranspiration, trees and damage to foundations in sensitive clays. *Can. Geotechnical Conference*. 2, 533-538

Smethurst J. A., Clarke D. and Powrie W. 2006 Seasonal changes in pore water pressure in a grass-covered cut slope in London clay. *Geotechnique*. 56, 523-537

Tamrakar S. B., Toyosawa Y., Mitachi T. and Itoh K. 2005 Tensile strength of compacted and saturated soils using newly developed tensile strength measuring apparatus. *Soils and Foundations*, 45 (6), 103-110

Tomlinson M. J. 2001 Foundation design and construction. 7th ed. Pearson Education, Harlow, England

Trabelsi H., Jamei M., Zenzri H. and Olivella S. 2011 Crack patterns in clayey soils: Experiments and modelling. *Int. J. Numerical and Analytical Methods in Geomech.,* 36 (11), 1410-1433

van Genuchten M. T. 1980 A closed-form equation for predicting the hydraulic conductivity of unsaturated soils. *J. Soil Soc. Am*. 44 (5), 892-898